Spatial gene expression and functional network abnormalities in multiple sclerosis: exploring biological influence on brain functional reorganization

[1,2,3]Paolo Preziosa, [1,2]Matteo Azzimonti, [1]Loredana Storelli, [1]Paola Valsasina, [1,3]Nicolò Tedone, [1,2,4]Monica Margoni, [1]Lucrezia Rossi, [1,2,3]Maria A. Rocca, [1,2,3,4,5]Massimo Filippi

P192

[1]*Neuroimaging Research Unit, Division of Neuroscience, IRCCS San Raffaele Scientific Institute, Milan, Italy;* [2]*Neurology Unit, IRCCS San Raffaele Scientific Institute, Milan, Italy;* [3]*Vita-Salute San Raffaele University, Milan, Italy;* [4]*Neurorehabilitation Unit, IRCCS San Raffaele Scientific Institute, Milan, Italy;* [5]*Neurophysiology Service, IRCCS San Raffaele Scientific Institute, Milan, Italy.*

INTRODUCTION and PURPOSE

Functional magnetic resonance imaging (fMRI) studies have shown that resting-state (RS) functional connectivity (FC) reorganization accompanies multiple sclerosis (MS) progression, with early compensatory increases followed by heterogeneous and potentially maladaptive patterns linked to disability and cognitive impairment [1]. Graph-theory approaches, particularly voxel-wise degree centrality, have revealed network-specific alterations: reduced centrality in the sensorimotor and salience networks relates to motor and cognitive dysfunction, while increased centrality in the default-mode network (DMN) reflects maladaptive hub overload [1]. However, the biological mechanisms driving these functional network changes and their spatial distribution remain poorly understood. Recent advances in brain-wide transcriptomic atlases, such as the Allen Human Brain Atlas (AHBA), provide an opportunity to investigate whether intrinsic gene expression patterns influence regional vulnerability or resilience to MS-related network reorganization [2,3]. Linking transcriptomic data to imaging abnormalities may offer novel insights into the molecular underpinnings of functional plasticity and network collapse in MS.

The aim of this study was to identify regional abnormalities in degree centrality in a large cohort of MS patients compared with healthy controls (HC), and to explore spatial correlations between these functional network alterations and normative brain-wide gene expression patterns from the AHBA. We also investigated whether specific clinical phenotypes and cognitive status were associated with distinct gene–network relationships.

METHODS

- **Subjects.** 558 MS patients and 214 HC.
- **Neurological evaluation.** Disease duration, EDSS score, MS clinical phenotype (relapsing-remitting [RR]; progressive [P]), ongoing disease modifying treatment (DMT).
- **Neuropsychological evaluation.** Cognitive performance: Brief Repeatable Battery of Neuropsychological tests (BRB-N). Global cognitive impairment: ≥2 impaired cognitive domains (≥1 test of BRB-N assessing that domain with a score 1.5 standard deviations below normative values). Cognitive impairment in specific domains (information processing speed/attention, verbal memory, visual memory and verbal fluency): ≥1 abnormal neuropsychological tests of BRB-N for each domain.
- **Brain MRI acquisition and MRI analysis (3.0 Tesla scanners).**
  - Dual-echo (DE) turbo spin echo sequence (Protocol I) or 3D fluid-attenuated inversion recovery (FLAIR) (Protocol II): quantification of T2-hyperintense white matter (WM) lesion volume (LV) using Jim 8.0, Xinapse Systems Ltd, Colchester, UK and an in-house implemented method.
  - 3D T1-weighted fast field echo (Scanner 1) or 3D T1-weighted turbo field echo (Scanner 2): after lesion filling, quantification of normalized brain (NBV), cortical (NcGMV), deep gray matter (GM) (NDGMV) and WM (NWMV) volumes using FSL SIENAx2.
  - T2*-weighted echo planar imaging sequence for RS fMRI: 200 images for Protocol I and 320 images for Protocol II. RS fMRI data were preprocessed with the CONN toolbox. Images were realigned, registered to lesion-filled 3D T1-weighted scans, normalized to Montreal Neurological Institute (MNI) space (SPM12), visually checked, and smoothed (6 mm Full Width at Half Maximum [FWHM]). Noise correction included aCompCor with CSF/WM components, motion parameters with derivatives, ART-detected outliers, and initial volumes; data were then detrended and band-pass filtered (0.01–0.1 Hz).Voxel-wise degree centrality maps were computed using Resting-State fMRI Data Analysis Toolkit – Degree Centrality (REST-DC). Centrality was defined as the number of suprathreshold positive correlations (r>0.25) each GM voxel had with all others, excluding WM/non-signal voxels. Maps were Fisher Z-transformed to reduce variability.
- **Spatial association with gene expression.**
  - Brain-wide transcriptomic data were obtained from the AHBA. A list of 3,634 MS-related genes was selected using the OpenTargets platform. Preprocessing steps included representative probe selection, z-score normalization across donors, and restriction to the left hemisphere to minimize sampling bias.
  - Spatial correlations between centrality abnormalities (t-maps) and gene expression profiles were assessed with the **MENGA** platform [4]. Weighted regression models used principal component analysis (PCA)-derived gene components (≥95% variance explained) to prevent overfitting. Reliability was confirmed by bootstrapping (1,000 resamples) and donor auto-correlation analysis. The adjusted R^2 indicated the variance in centrality abnormalities explained by gene expression, with chance likelihoods used to assess robustness.
- **Enrichment and cell-type analyses.**
  - Genes showing significant and reliable spatial associations with centrality abnormalities (R^2≥0.15; chance likelihood <0.001; auto-correlation ≥0.2) were submitted to functional enrichment using the ToppGene Suite. Overrepresented Gene Ontology (GO) categories were identified across molecular functions, biological processes, and cellular components, with significance assessed by Bonferroni-corrected hypergeometric tests (p<0.05).
  - To determine cellular specificity, gene expression was further explored using the celltypes.org/brain R/Shiny platform with the single-cell human brain transcriptome dataset from Darmanis et al. [5]. Expression was quantified across CNS cell types (neurons, astrocytes, microglia, endothelial cells, etc.) using measures of specificity, enrichment, and absolute expression, normalized with the quantile method.

RESULTS

Demographic, clinical, neuropsychological and structural MRI analysis

•**Table 1** shows the main demographic, clinical and structural MRI characteristics of HC and MS patients and of MS patients according to their clinical phenotype and the presence of cognitive impairment.

Table 1.	HC (n=214)	MS (n=558)	p	Clinical phenotype		p	Cognitive impairment		p
				RRMS (n=365)	PMS (n=193)		Co-P MS (n=347)	Co-I MS (n=144)	
Median age (IQR) years]	38.4 (27.4;50.9)	42.4 (33.3;50.6)	0.008	37.9 (29.3;45.2)	49.9 (43.7;57.7)	<0.001	41.8 (31.2;48.8)	44.9 (36.7;54.4)	0.002
Sex: Female/Male	116/98	342/216	0.073	230/135	112/81	0.250	214/133	79/65	0.161
Median education (IQR) [years]	16.0 (13.0;18.0)	13.0 (13.0;16.0)	<0.001	13.0 (13.0;17.0)	13.0 (10.0;13.0)	<0.001	13.0 (13.0;17.0)	13.0 (10.0;13.0)	<0.001
Median DD (IQR) [years]	-	11.5 (4.1;18.0)	-	8.0 (2.5;14.0)	17.7 (12.0;23.4)	<0.001	10.1 (3.4;17.6)	14.4 (6.3;21.6)	<0.001
Clinical phenotype	-	365 RR; 193 P	-	365 RR	133 SP; 60 PP	-	245 RR; 69 SP; 33 PP	62 RR; 58 SP; 24 PP	<0.001
Median EDSS (IQR)	-	2.5 (1.5;5.5)	-	2.0 (1.5;3.5)	6.0 (5.0;7.0)	<0.001	2.0 (1.0;4.5)	4.5 (2.5;6.0)	<0.001
DMT*: None/MET/HET	-	143/276/139	-	63/211/91	80/65/48	<0.001	86/169/92	45/63/36	0.331
Scanner [Achieva/Ingenia]	110/104	334/224	0.033	228/137	106/87	0.084	187/160	86/58	0.236
Median brain T2 LV[a] (IQR) [ml]	0.00 (0.00;0.14)	4.01 (1.52;9.91)	<0.001	2.92 (1.12;6.80)	8.54 (3.34;18.64)	<0.001	3.30 (1.27;6.90)	10.61 (3.69;20.48)	<0.001
EM NBV (SE) [ml]	1581 (4)	1532 (3)	<0.001	1543 (4)	1504 (5.3)	<0.001	1545 (3)	1496 (5)	<0.001
EM NcGMV (SE) [ml]	640 (3)	614 (3)	<0.001	617 (3)	602 (3.7)	0.001	616 (2)	593 (4)	<0.001
EM NDGMV (SE) [ml]	55.3 (0.3)	51.0 (0.2)	<0.001	52.2 (0.3)	48.5 (0.4)	<0.001	52.2 (0.3)	47.7 (0.4)	<0.001
EM NWMV (SE) [ml]	745 (3)	722 (2)	<0.001	728 (2)	711 (3.4)	<0.001	734 (2)	710 (3)	<0.001

Comparisons performed using Chi square test (sex, scanner, clinical phenotype, DMT) and Mann-Whitney U test (age, education, disease duration, EDSS). Sex-, age- and scanner-adjusted linear models were applied for MRI features.
*MET: interferon beta, glatiramer acetate, teriflunomide, dimethyl fumarate; HET: fingolimod, siponimod, cladribine, natalizumab, ocrelizumab. [a]comparison performed on log scale.
Abbreviations: Co-I=cognitively impaired; Co-P=cognitively preserved; EM=estimated mean; HET=high efficacy treatment; IQR=interquartile range; MET=moderate efficacy treatment; ml=millilitre; SE=standard error.

Patterns of degree centrality abnormalities, spatial correlations with gene expression and enrichment analysis

- *MS patients vs. HC*
  - **Higher centrality** in the bilateral precuneus, bilateral orbitofrontal and inferior temporal cortices (regions part of the DMN) (**Figure 1**), showing significant spatial correlation with the expression of 17 genes (p<0.001). Enrichment analysis revealed overrepresentation of calcium signaling, cell migration, and immune system pathways (**Table 2**). Migration-related genes, mainly expressed in neurons, microglia, and endothelial cells, are implicated in different CNS and immune system functions, including resolution of inflammation and damage repair.
  - **Lower centrality** in the bilateral insula (a key region of the salience network [SN]), and in the left and right cerebellum (crus I, lobules VI-IX) (p<0.001, uncorrected) (**Figure 1**), showing significant spatial correlation with the expression of 10 genes (p<0.001). These genes were enriched for cytokine response processes (p=0.046, Bonferroni corrected), indicating that higher pro-inflammatory cytokine expression may underlie reduced centrality. Expression was predominant in astrocytes, endothelial cells, and neurons (**Figure 2**).

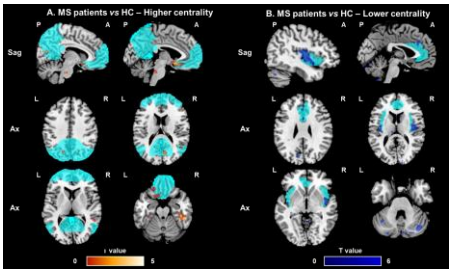

Figure 1. SPM12 analysis showing voxel-wise differences in centrality between MS patients and HC; clusters of higher centrality in MS patients are shown in red-yellow scale (A), while clusters of lower centrality are shown in blue-light blue scale (B); images are thresholded at p<0.001, uncorrected, cluster extent k=20. Results are superimposed on the MNI152 atlas and overlaid on a standard template mask of the DMN (cyan) for higher centrality, and on a standard template of the SN (cyan) for lower centrality. Abbreviations: A=anterior; Ax=axial; L=left; R=right; P=posterior; Sag=sagittal.

Centrality abnormalities	GO terms	ID	Name	p	Bonferroni	N of genes
MS vs. HC: Higher centrality	Molecular function	GO:0004683	Calmodulin-dependent protein kinase activity	<0.001	0.036	2
	Biological process	GO:0060374	Mast cell differentiation	<0.001	0.023	2
		GO:0030334	Regulation of cell migration	<0.001	0.046	7
MS vs. HC: Lower centrality	Molecular function	GO:0034097	Response to cytokine	<0.001	0.046	5
		GO:0003682	Chromatin binding	<0.001	0.014	5
		GO:0008327	Methyl-CpG binding	<0.001	0.028	2
		GO:0043021	Ribonucleoprotein complex binding	<0.001	0.048	3
PMS vs. RRMS and HC: Higher centrality	Biological process	GO:0040029	Epigenetic regulation of gene expression	<0.001	0.028	4
		GO:0006338	Chromatin remodelling	<0.001	0.045	5
	Cellular component	GO:0045120	Pronucleus	<0.001	0.014	2
		GO:0005721	Pericentric heterochromatin	<0.001	0.019	2
		GO:0005759	Mitochondrial matrix	<0.001	0.029	4

Table 2. Enrichment analysis showing significantly overexpressed pathways (molecular function, biological processes, cellular components) among genes showing spatial association with centrality abnormalities in MS patients, also according to clinical phenotype. Abbreviations: GO=gene ontology; ID=identification.

- *MS clinical phenotypes*
  - PMS vs. RRMS and HC: **higher centrality** in the precuneus and angular gyrus (part of the DMN), in the right and left cerebellum (lobules VI-VIII-IX) and orbitofrontal cortex (p<0.001, uncorrected) (**Figure 2**). This pattern was correlated with the physiological expression of 14 genes (p<0.001), enriched for epigenetic regulation pathways. Four genes encoded mitochondrial matrix proteins (p=0.029, Bonferroni corrected), suggesting their involvement in mitochondrial energy production. These genes showed ubiquitous CNS expression. PMS patients also showed **lower centrality** in bilateral insula and anterior cingulate cortex, as well as the thalamus bilaterally and the right caudate nucleus (p<0.001, uncorrected), with no significant spatial associations with transcriptomic data.
  - RRMS vs. PMS and HC: no significant suprathreshold cluster in the conjunction analysis.

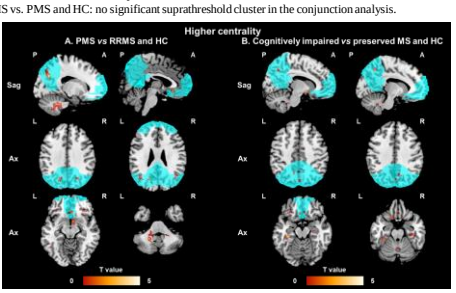

Figure 2. SPM12 analysis showing voxel-wise differences in centrality between MS patients, according to their clinical phenotype and cognitive status, and HC. (A) Higher centrality in PPMS vs. RRMS and HC; (B) Higher centrality in cognitively impaired MS patients vs. cognitively preserved and HC. Clusters of higher centrality are shown in red-yellow scale; images are thresholded at p<0.001, uncorrected, cluster extent k=20. Results are superimposed on the MNI152 atlas and overlaid on a standard template mask of the DMN (cyan). Abbreviations: A=anterior; Ax=axial; L=left; R=right; P=posterior; Sag=sagittal.

- *Cognition*
  - Co-I vs. Co-P and HC: **higher centrality** in bilateral mesial temporal lobe regions, the right and left precuneus (part of the DMN) and the orbitofrontal cortex (p<0.001, uncorrected) (**Figure 2**). This pattern was negatively associated with the expression of 2 genes, *DNASE1* and *CP* (p<0.001). *DNASE1* encodes for an enzyme involved in deoxyribonucleic acid (DNA) degradation, which may play a role in neuronal apoptosis. It is predominantly expressed in neurons and astrocytes. *CP* encodes for ceruloplasmin, a protein involved in iron homeostasis in the CNS and ubiquitously expressed among CNS cell types. Co-I MS also showed small clusters of **lower centrality** in left and right thalamus, left insula, left precentral gyrus and right postcentral gyrus (p<0.001, uncorrected), with no significant spatial associations with transcriptomic data.
  - Co-P MS vs. Co-I MS and HC: no significant suprathreshold centrality clusters in the conjunction analysis.

CONCLUSIONS

- **MS patients showed increased centrality in regions part of the DMN and lower centrality in regions of the SN and cerebellum, reflecting maladaptive hub overload and network disconnection.**
- **DMN alterations correlated with genes resolution of inflammation and damage repair, whereas SN/cerebellar decreases aligned with cytokine signaling genes, suggesting region-specific vulnerability.**
- **PMS patients exhibited more pronounced DMN centrality increases linked to epigenetic regulation and mitochondrial function, highlighting maladaptive but metabolically supported hub reorganization.**
- **Cognitive impairment was associated with DMN and mesial temporal hyperconnectivity, linked to lower expression of *DNASE1* (apoptotic clearance) and *CP* (iron metabolism), pointing to mechanisms of neurodegeneration.**
- **Physiological regional gene expression spatially correlates with MS-related functional network alterations. Inherent biological factors may influence regional vulnerability or resilience to MS pathology, ultimately affecting functional reorganization.**

REFERENCES

[1] Rocca et al., Neuroimage Clin 2022
[2] Hawrylycz et al., Nature 2012
[3] Preziosa et al., Mol Psy 2024
[4] Rizzo et al., PLoS One 2016
[5] Darmanis et al., PNAS 2015